International Journal of Pharmaceutics 602 (2021) 120639

Contents lists available at ScienceDirect

International Journal of Pharmaceutics

journal homepage: www.elsevier.com/locate/ijpharm

Melt extrusion deposition (MED™) 3D printing technology – A paradigm shift in design and development of modified release drug products

Yu Zheng [a,*], Feihuang Deng [a], Bo Wang [a], Yue Wu [a], Qing Luo [a], Xianghao Zuo [a], Xin Liu [a], Lihua Cao [a], Min Li [a], Haohui Lu [a], Senping Cheng [a], Xiaoling Li [a,b,*]

[a] Triastek, Inc., 12 East Mozhou Road, U Park P402, Nanjing, Jiangsu, China
[b] Department of Pharmaceutics and Medicinal Chemistry, Thomas J. Long School of Pharmacy, University of the Pacific, 3601 Pacific Ave, Stockton, CA, United States

ARTICLE INFO

Keywords:
Three-dimensional (3D) printing
Melt Extrusion Deposition (MED™)
Modified release
3D printing formulation by design (3DPFbD®)
Pharmaceutics
Drug delivery systems

ABSTRACT

Three-dimensional printing (3DP) technology offers unique advantages for pharmaceutical applications. However, most of current 3D printing methods and instrumentations are not specifically designed and developed for pharmaceutical applications. To meet the needs in pharmaceutical applications for precision, compatibility with a wide range of pharmaceutical excipients and drug materials without additional processing, high throughput and GMP compliance, an extrusion-based 3D printer based on Melt Extrusion Deposition (MED™) 3D printing technology was developed in this study. This technology can process powder pharmaceutical excipients and drugs directly without the need of preparing filament as required by FDM 3D printing. Six different tablet designs based on compartment models were used to demonstrate the precision and reproducibility of this technology. The designed tablets were fabricated using the GMP-compliant MED™ 3D printer and were evaluated *in vitro* for drug release and *in vivo* for selected designs using male beagle dogs. Tablet designs with one or more compartments showed versatile release characteristics in modulating the release onset time, release kinetics, duration of release and mode of release. Multiple drugs or formulations were fabricated into a single tablet to achieve independent release kinetics for each drug or to fine-tune the pharmacokinetic profile of a drug. Building upon the theoretical analysis of models, precision and reproducibility of MED™ 3D printing technology, a novel product development approach, 3D printing formulation by design (3DPFbD®) was developed to provide an efficient tool for fast and efficient pharmaceutical product development. The MED™ 3D printing represents a novel and promising technology platform encompassing design and development of modified drug release products and has potential to impact the drug delivery and pharmaceutical product development.

1. Introduction

Three-dimensional (3D) printing is capable of creating objects with complex 3D structures based on digital models, thereby providing unique opportunities in the development of pharmaceutical products. The computer-controlled layer-by-layer formation process of 3D printing provides a tool for pharmaceutical scientists to create the functionality of drug delivery system beyond the current methods can do and enables the delivery system to tailor virtually any desired release profile to achieve a pharmacokinetic profile that meets the patient's clinical needs. With the structures built by 3D printing in delivery systems, the release of active ingredients can be modulated by simply varying their geometries and/or printing parameters using the same material feedstocks as employed in conventional tablets. The versatility of creating drug delivery systems using 3D printing offers an exciting opportunity for pharmaceutical scientists and could revolutionize the design and fabrication of solid dosage forms, such as tablets. In addition to creating novel drug delivery systems, the pharmaceutical applications of 3D printing also has potential for use in individualized dosing [1,2] by utilizing its flexible and quick formation features for creating at the point of care dosage forms with doses customized for an individual patient, although the regulatory aspects for widely deployment of individualized dosing using 3D printing technology are yet to be clearly defined.

Michael Cima of the Massachusetts Institute of Technology was the first to adapt 3DP for pharmaceutical applications [3,4]. In the past decade, the application of 3D printing technology has been the subject of significant interest among pharmaceutical scientists. Various 3D

* Corresponding authors.
E-mail addresses: yzheng@triastek.com (Y. Zheng), xli@pacific.edu (X. Li).

https://doi.org/10.1016/j.ijpharm.2021.120639
Received 11 January 2021; Received in revised form 19 April 2021; Accepted 20 April 2021
Available online 24 April 2021

printing technologies, such as binder jetting, material extrusion, material jetting, powder bed fusion, and VAT photopolymerization have been explored for pharmaceutical applications [1–14]. For example, drug release rates have been varied by either altering the infill parameters [5,7,8], or changing the shape, size, and surface area of the drug-containing component in 3D printed dosage forms [6,9,11]. For 3D printed capsules with a core–shell structure, release onset time from the core has been controlled by altering the thickness of an erodible outer shell [15]. Such an outer shell can also be comprised of a pH-responsive material, as with conventional enteric-coated tablets, thereby causing drug to release after passing through the stomach [16]. The feasibility of combining multiple active ingredients, sometimes with differing pharmacokinetics or release characteristics, has been demonstrated by creating multi-layer or multi-compartmental polypill formulations using selective laser sintering (SLS) [12], fused deposition modelling (FDM) [17], or material extrusion-based 3D printing technologies [18,19]. Among the various 3D printing technologies mentioned above, fused deposition modeling has been the most evaluated method for pharmaceutical applications due to its low-cost and relatively high resolution, as well as compatibility with a relatively wide selection of pharmaceutical grade/GRAS excipients that can be adapted for printing. FDM method requires time-consuming filament processing developments that limited the choice of pharmaceutical excipients and also diminished the rapid prototyping advantage of 3D printing (3DP) for early-stage drug development.

The existing 3D printing technologies and printers are not specifically designed for pharmaceutical use, and there are several disadvantages that need to be overcome before the extensive application of 3D printing technologies can be realized in the pharmaceutical areas. There is a need to design and develop 3D printing method and equipment specifically for pharmaceutical applications. The needs in pharmaceutical applications for the 3D printers include precision and accuracy of each printed unit, reproducibility, use of pharmaceutic excipients without additional processing, coordination of printing multiple materials, high throughput and good manufacturing practice (GMP) compliance. Currently, Aprecia, Triastek and FabRx have developed GMP-compliant 3D printers specifically for pharmaceutical applications. Triastek and FabRx independently developed novel material extrusion-based 3D printing technologies using powdered starting materials to eliminate the burden of filament preparation [20,21].

The ability to control dose, drug release rate, onset time, site of release, and mode of release within a dosage form can provide significant advantages in the development of new oral drug products as the control of these factors can deliver the right amount of drug at the right time in the right GI location(s) to optimize therapeutic outcomes. Individualized dosing also has the potential to develop tailor-made dosage forms with customizable dose and release profiles specifically for a specific patient. Additionally, the ability to incorporate multiple drugs independently in a tablet, particularly when these drugs require different release kinetics or have compatibility issues can provide substantial therapeutic and product development advantages. In these circumstances, the capability of multi-material printing presents new possibilities in creating different functional structures inside the dosage form to achieve the aforementioned drug design options, rather than simply changing infill pattern or infill density. Due to the limited flexibility of commercial FDM printers in creating complex internal structures using multiple materials, many researchers have explored complicated fabrication methods to circumvent these instrumentation limitations, for example, by combining FDM printing with injection molding [22], injection filling [15], or manual dispensing [23] to achieve programmed drug release characteristics and/or to combine multiple drugs in the same dosage forms with independent release characteristics. The design of multi-material 3D printers can potentially obviate these complicated fabrication methods. Heretofore, FabRx and DiHeSys Digital Health Systems GmbH, have developed material extrusion-based pharmaceutical 3D printers that can adapt 3 and 4 nozzles, respectively, for flexible preparation of personalized medicines [24].

In additional to the capability of handling multiple materials, the output of current commercially available extrusion-based 3D printers is mostly limited to print one tablet at a time. Although it may meet the need in individualized dosing, it is obvious that the output is not suitable for the mass production of drug products. For research development and production of pharmaceutical products, a scalable extrusion-based pharmaceutical 3D printing system that can be used from preclinical stage to manufacturing of commercial products will facilitate the seamless translation from early-phase development to commercial manufacturing.

As such, the objective of this report was to introduce an innovative 3D printing technology, Melt Extrusion Deposition (MED™) that converts powder feedstocks into softened/molten states followed by precise layer-by-layer deposition to produce objects with desired internal geometric structures. Based on MED™ technology, a GMP-compliant MED™ 3D printer with multiple printing stations has been designed to enable precise fabrication of multi-component tablets with designed structures that allow wide range of control over drug release kinetics and modes. The advantages of MED™ 3D printing technology were demonstrated by using a novel product development approach, 3D printing formulation by design (3DPFbD®), for enabling an efficient drug product development process.

2. Materials and methods

2.1. Materials

The materials used in the study were as follows: metoprolol succinate (Yung Zip Chemical Ind. Co., Ltd., Taiwan), tofacitinib citrate (MSN Laboratories Private Ltd., India), levodopa and carbidopa (Yuancheng Gongchuang Technology Co., Ltd., Wuhan, China), topiramate (Scino-Pharm Taiwan, Ltd., Taiwan), clonidine hydrochloride (PCAS Finland Oy, FI-20101 Turku, Finland), ammonio methacrylate copolymer type B (Eudragit® RS PO, Evonik Nutrition & Care GMBH, Darmstadt, Germany), hydroxypropyl cellulose (HPC Klucel™ EF & JF, Ashland Specialty Ingredients, DE, USA), hydroxypropyl methylcellulose acetate succinate (AquaSolve™ HPMC-AS LG & HG, Ashland Specialty Ingredients, DE, USA), ethyl cellulose, (Aqualon™ EC-N10 Pharm, Ashland Specialty Ingredients, VA, USA), vinylpyrrolidone vinyl acetate copolymer (Kollidon® VA64, BASF SE, Ludwigshafen, Germany), polyethylene glycol (PEG 400 & 8000, Dow Chemical Pacific Ltd., LA, USA), polyethylene glycol (PEG 1500, Aladdin Biochemical Technology Co., Ltd., Shanghai, China), stearic acid (Hesego Industry Sdn Bhd, Selangor, Malaysia), triethyl citrate (Vertellus LLC, NC, USA), croscarmellose sodium (DMV-Fonterra Excipients GmbH & Co, Foxhol, Netherlands). HPLC solvents and dissolution media reagents were of analytical grade.

2.2. Design of MED™ 3D printed tablets

SOLIDWORKS® Professional 2019 SP4.0 (Dassault Systèmes, France) was used to create the structure of tablets and exported as stereolithography (.stl) files. All tablets were designed based on the compartment models with a core–shell structure where one or more drug release compartments are housed in an impermeable shell with only one API containing side being exposed to the surrounding medium.

A series of tablets (A1-A6) containing a multilayered drug compartment were designed with different surface area and height of the layers (Fig. 1) to produce different release profiles. The amount of drug released over a given time can be controlled by varying the surface area and the height of the layer. The surface area and height for each layer in the drug compartment of Design A are described in Table 1.

For Designs B and C, a layer of either erodible material or pH-responsive material, respectively, was added. Fig. 2 depicts the compartmental Design B with an erodible delay layer on top of a

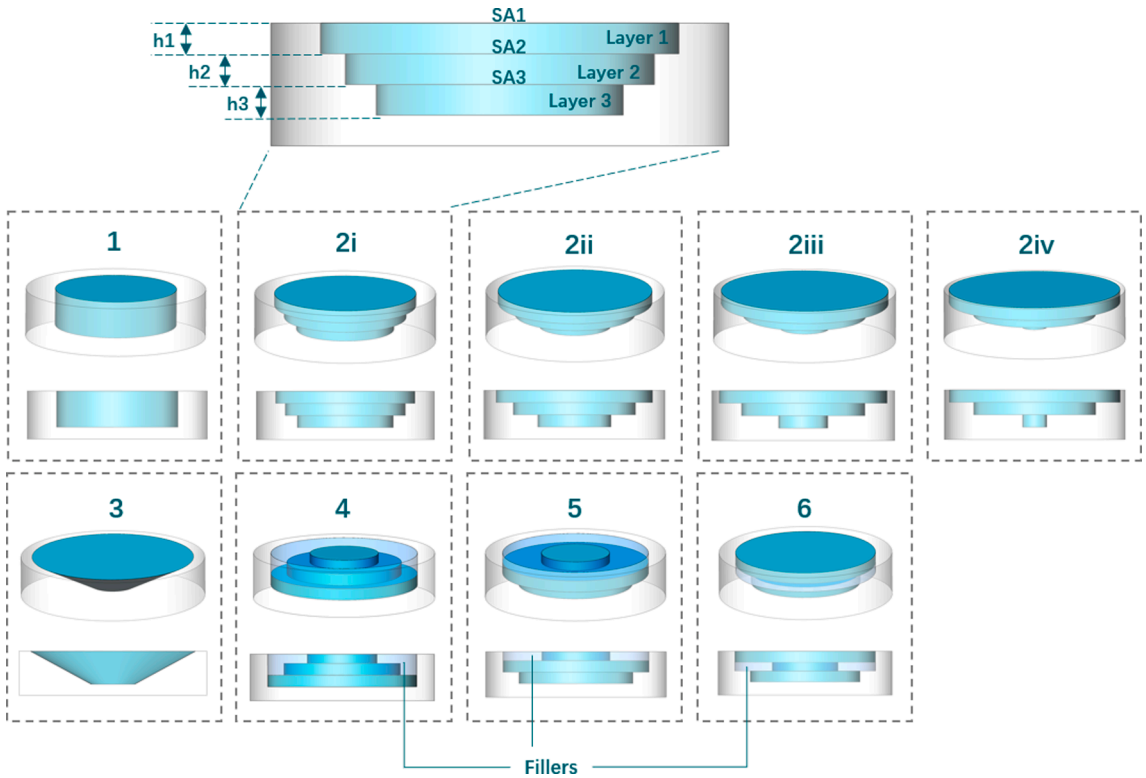

Fig. 1. Design A: Multilayered drug compartment in core–shell structure tablets with constant or varied surface area (SA). Drug compartment (teal), shell (pale white), fillers (bluish). (1) Drug compartment with constant SA. (2) Drug compartment with stepwise decreasing SA. (3) Drug compartment with continuous decreasing SA. (4) Drug compartment with stepwise increasing SA. (5) Drug compartment with increasing–decreasing SA. (6) Drug compartment with decreasing-increasing SA.

Table 1
Structural parameters of MED™ 3D printed tablets with multilayered drug compartment.

Design A	Trend of surface area exposed	Layer 1	Layer 2	Layer 3	Height of layer (mm)
		Surface area (SA, mm^2)			
1	Constant	25π	25π	25π	$h_1 = h_2 = h_3 = 1$
2i	Stepwise decreasing	33.64π	25π	16π	$h_1 = h_2 = h_3 = 1$
2ii	Stepwise decreasing	40.96π	25π	9π	$h_1 = h_2 = h_3 = 1$
2iii	Stepwise decreasing	46.24π	25π	4π	$h_1 = h_2 = h_3 = 1$
2iv	Stepwise decreasing	49π	25π	π	$h_1 = h_2 = h_3 = 1$
3	Continuous decreasing	56.25π	–	4π	$h = 3$
4	Stepwise increasing	9π	25π	40.96π	$h_1 = 0.8, h_2 = h_3 = 1$
5	Increasing-decreasing	9π	40.96π	25π	$h_1 = 0.8, h_2 = h_3 = 1$
6	Decreasing-increasing	40.96π	9π	25π	$h_1 = h_3 = 1, h_2 = 0.8$

cylindrical drug compartment. The thickness of the delay layers evaluated ranged from 0 to 0.4 mm. For Design C, a pH-responsive layer was designed for drug release at either pH 5.8 or 6.8, as shown in Fig. 3.

Design D was constructed with different APIs placed in different compartments and configured to release at different rates. As depicted in Fig. 4, an immediate release (IR) formulation consisting of tofacitinib (11 mg) and an extended release (ER) formulation consisting of metoprolol (25 mg) were combined in a single tablet constructed with three compartments. Formulation of metoprolol was incorporated into compartment 1, while formulations containing 42% and 58% of the dose of tofacitinib were incorporated into compartments 2 and 3, respectively. A delay layer was used to seal compartment 3 to acquire a two-pulse release profile for metoprolol. All compartments are physically isolated by shell material for independent release.

For Design E and F, immediate release (IR) and extended release (ER) components of the same drug were combined in one or separate compartments in a single tablet. As depicted in Fig. 5, immediate release (IR) formulation and extended release (ER) formulation consisting of a total of 70 mg of levodopa were combined in Design E tablet constructed with two compartments. For Design F, IR formulation and ER formulation of topiramate (100 mg) were layered in single compartment for sequential release, as shown in Fig. 6.

2.3. Simulation of drug release profiles

For Design A tablets (variable layer thickness and surface area design), the theoretical release percentage Q(t)% with time (t) can be expressed using a general equation:

$$Q(t)\% = \frac{D_{(t)}}{D_{total}} = \frac{R_D \int_0^t S(t)dt}{V} \times 100\% \quad (1)$$

where $D_t$is the amount of drug released from the drug compartment at time t, $D_{total}$is the total dose contained in the drug compartment, R_D is the matrix dissolution rate in depth per unit time, t is the dissolution time, $S_{(t)}$ is the exposed surface area of drug compartment at time t, and V is the total volume of the drug compartment. The volume of matrix within which the drug is dissolved at a specific time t is expressed as the integration of the exposed surface area of the drug compartment over time and multiplying by the dissolution rate. The release percentage Q (t)% at time t is then calculated by dividing volume within which the drug is dissolved by the total volume of the drug compartment. The

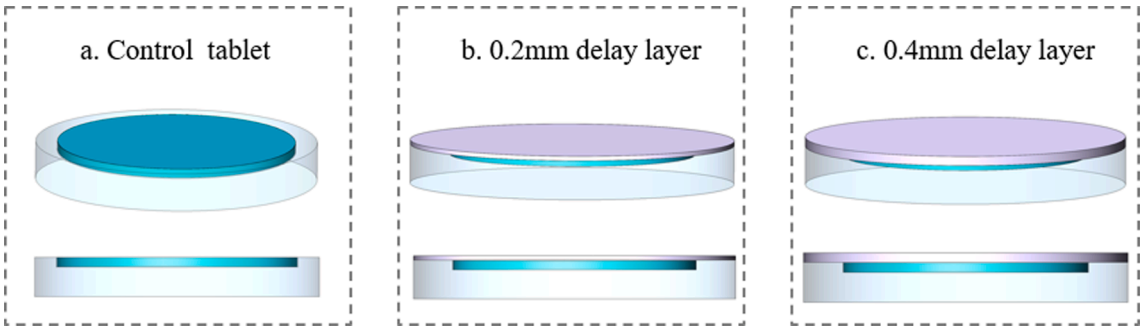

Fig. 2. Design B: modified release tablets with and without a delay layer. Shell (pale white), drug core (teal), delay layer (lavender). (a) Tablet without a delay layer. (b) Tablet with a 0.2 mm delay layer. (c) Tablet with a 0.4 mm delay layer.

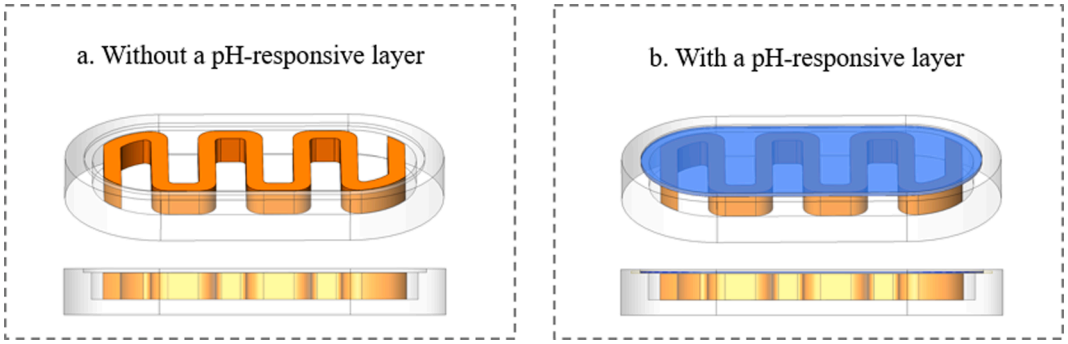

Fig. 3. Design C: modified release tablets with and without a pH-responsive layer. Shell (pale white), drug core (orange), pH-responsive layer (transparent blue). (a) Tablet without a pH-responsive layer. (b) Tablet with a 0.1 mm pH-responsive layer.

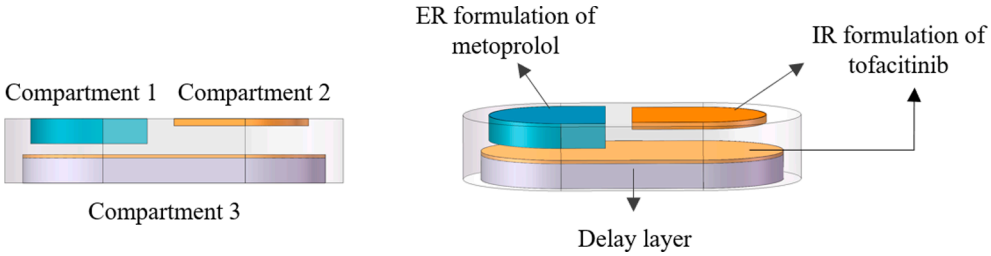

Fig. 4. Design D: multi-compartment tablets for independent release of drug combination. Shell (pale white), IR formulation of tofacitinib (orange), delay layer (lavender), ER formulation of metoprolol (teal).

Fig. 5. Design E: multi-compartment tablets for concurrent release of IR formulation and ER formulation. Shell (pale white), IR formulation of levodopa (orange), ER formulation of levodopa (teal).

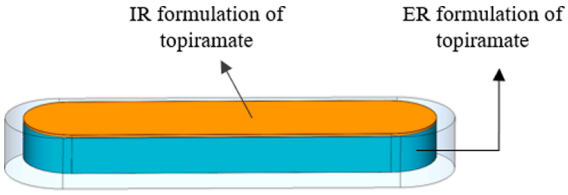

Fig. 6. Design F: single-compartment tablets for sequential release of IR formulation and ER formulation. Shell (pale white), IR formulation of topiramate (orange), ER formulation of topiramate (teal).

assumption for Eq (1) is that the rate of drug released from the drug-containing matrix is equal to the rate of dissolution within the matrix.

For a gradually decreasing surface area of the drug compartment in the Design A3 tablet, the radii of the top and bottom surfaces were set as r_1 and r_2 respectively ($r_1 > r_2$), and the total thickness of the drug compartment as h. At a specific time t, the height of the dissolved drug compartment is equal to $R_D \cdot t$, and the radius of the dissolution front is equal to $\frac{r_2 - r_1}{h} \cdot R_D \cdot t + r_1$. Therefore, the cumulative release percentage Q(t)% can be presented using the following equation:

$$Q(t)\% = \frac{AB^2}{3}t^3 + ABRt^2 + AR^2t \quad (2)$$

where $A = \frac{\pi \cdot R_D}{V}$, $B = \frac{r - R}{h} \cdot R_D$.

For a constant surface area, Design A1 tablet the release percentage Q(t)% at time t can be expressed by:

$$Q(t)\% = AR^2t \times 100\% \quad (3)$$

For Designs A2 and A4-A6 tablets that are configured with a stepwise change in surface area for the drug compartment, their drug compartment can be treated as sequentially stacked multiple cylindrical drug compartments with varying surface areas, and the cumulative release percentage Q(t)% at time t can be expressed using the following equation:

$$\mathrm{Q(t)}\% = \frac{R_D}{V}\cdot\left(\int_0^{t_1} S_1 dt + \int_{t_1}^{t_1+t_2} S_2 dt + \cdots + \int_{\sum_0^{n-1} t_n}^{\sum_1^{n} t_n} S_n dt\right) \times 100\% \quad (4)$$

where S_n and t_n are the surface area and dissolution duration of the specific drug layer n in the multilayered compartment, respectively, and$t_n = \frac{h_n}{R_D}$ where h_n is the thickness of the specific drug layer n in the multilayered compartment.

The similarity factors (*f2*) were used to assess similarity of *in vitro* drug release profiles and the simulated drug release profiles. The *f2* values were calculated using the following equation [25]:

$$f_2 = 50 \times \log\{[1 + \frac{1}{n}\sum_{t=1}^{n}(S_t - T_t)^2]^{-0.5} \times 100\} \quad (5)$$

where n represents the time points, S_t and T_t are the cumulative drug release rate of the simulation and test sample at each time point, respectively.

2.4. Fabrication of tablets

As depicted in Fig. 7, a MED™ 3D printer is comprised of a material feeding and mixing module, a material conveying module, multiple high precision printing stations and an XYZ moving plate. The printer consists of multiple printing stations for handling different materials or active pharmaceutical ingredients (API), with each printing station containing either a single nozzle or an array of nozzles. The printing stations coordinate with each other to build a tablet with the desired design. Briefly, pharmaceutical grade excipients possessing the necessary physicochemical and rheological properties were chosen from a material database for construction of each part of the structure (i.e., core, shell, delay layer, etc., Table 2). The stereolithography (.stl) file of the designed structure was converted into a G-Code file using slicer software (Slic3r Prusa Edition v. 1.40.0, Germany). A proprietary D3 software program was used for conversion of this G-Code file to an NC-Code containing a customized print path and other parameters for MED™ 3D printing. API and pharmaceutical excipients were mixed and melted in the material feeding and mixing module with multiple temperature zones and conveyed into the high precision printing station. With precise temperature and pressure control, the molten/softened material was extruded through printer nozzles and then deposited onto the XYZ moving plate, layer-by-layer, to form tablets with the designed structures.

A concentric infill was used for printing of core and filler of Design A tablets. A rectilinear infill was used for the printing of shell, delay layer, pH-responsive layer, and core of Design B-F tablets, where a subsequent layer was offset by 90 degrees to the previous layer in the X-Y coordinate. Other printing parameters such as nozzle diameter, temperature setting, perimeter and infill speed, infill density, and layer thickness are summarized in Table 3. The print speeds utilized were dependent on the structure complexity, size of the designed tablet, and nozzle diameter and are also listed in Table 3. The time to print the tablet designs presented herein on the R&D scale MED™ printer ranged from 4 min to 10 min. The printing rate or throughput increases when the printing nozzle array is used. Print speeds of up to 25 mm/sec with high precision can be achieved.

For the preparation of the small quantity of tablets used in this study, some tablets were fabricated using a two-step process instead of continuous feeding of powder material. The materials were premixed through a twin-screw extruder and then filled into a feed cartridge. A cartridge-and-piston design was used in place of the twin-screw design depicted in Fig. 7. Formulations for all designs were screened in the preformulation to ensure the chemical and physical stability and compatibility prior to fabrication of the tablets used in this study.

2.5. In vitro dissolution of printed tablets

The *in vitro* drug release from the 3D printed tablets was evaluated using the USP-II dissolution setup consisting of an Agilent 708-DS dissolution apparatus operated at 37 ± 0.5 °C and a paddle speed of 50 rpm in 900 mL of release medium. For Design C tablets constructed with a pH-responsive layer, the tablets were evaluated at pH 1.2 for two hours, then switched to pH 5.8 for an additional two hours, and then finally placed in pH 7.2 buffer for two hours. For Design E and F tablets, the drug release study was carried out in pH 1.2 and pH 7.5 release media, respectively. For the remaining 3D printed tablet designs, the dissolution test was carried out in pH 6.8 phosphate buffer. Samples (2 mL) were withdrawn at predetermined time intervals and replenished with the same amount of fresh release medium. The concentration of drug contained in the collected samples was determined using HPLC-UV/RID (Agilent 1260 Infinity II). The HPLC methods are described in Table 4. The percentage of drug released at each time point was represented as mean ± standard deviation. All measurements were made in triplicate and sink conditions were maintained throughout the drug release study. For Design A tablets, the cumulative amounts of drug released were plotted against time and the slope of the regression line through the time points corresponding to the dissolution of a specific layer was calculated to obtain the dissolution rate (mg/h) of each layer.

2.6. In vivo pharmacokinetic studies

The *in vivo* pharmacokinetics of 3D printed tablets were evaluated in

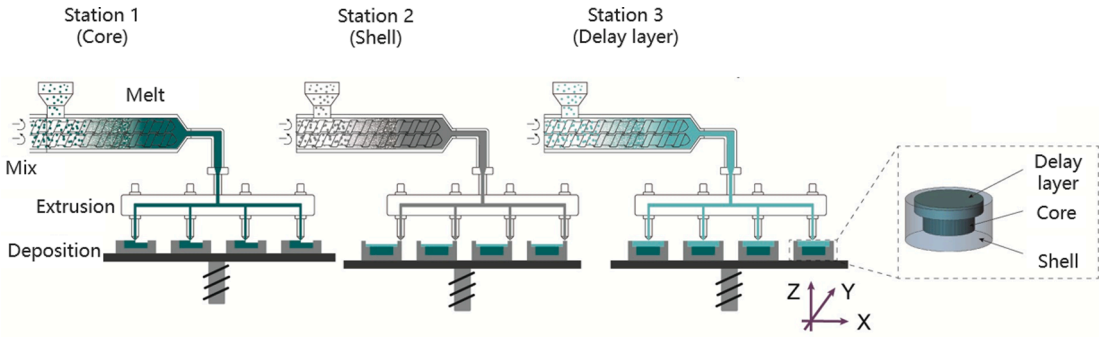

Fig. 7. Melt Extrusion Deposition (MED™) 3D printing process using multiple printing stations to coordinate the construction of core–shell structure tablets with a delay layer.

Table 2
Formulation Compositions of MED™ 3D Printed Design A-F Tablets.

			Components Ratio (% w/w)						
	Components	Function	A1, A2i-iv, A3-A6	A2v	B	C	D	E	F
Filler	HPC-EF	Matrix	85	–	–	–	–	–	–
	PEG 400	Plasticizer	15	–	–	–	–	–	–
Delay layer	HPC-EF	Matrix	–	–	90	–	85	–	–
	PEG 400	Plasticizer	–	–	10	–	–	–	–
	glycerol	Plasticizer	–	–	–	–	15	–	–
pH-responsive layer	HPMC-AS LG/HG	Matrix	–	–	–	75	–	–	–
	de-ionized water	Plasticizer	–	–	–	12.5	–	–	–
	triacetin	Plasticizer	–	–	–	12.5	–	–	–
Compartment 1	metoprolol	Model API	40	–	–	25	40	–	–
	tofacitinib	Model API	–	–	30	–	–	–	–
	levodopa/carbidopa	Model API	–	–	–	–	–	32/8	–
	topiramate	Model API	–	–	–	–	–	–	28
	clonidine	Model API	–	0.25	–	–	–	–	–
	HPC-JF	Matrix	40	79.8	–	–	40	35	–
	HPC-EF	Matrix	–	–	60	–	–	–	52
	Kollidon® VA 64	Matrix	–	–	–	60	–	–	–
	triethyl citrate	Plasticizer	–	19.95	–	–	–	–	–
	PEG 400	Plasticizer	20	–	10	15	20	25	20
Compartment2	tofacitinib	Model API	–	–	–	–	40	–	–
	levodopa/carbidopa	Model API	–	–	–	–	–	48/12	–
	topiramate	Model API	–	–	–	–	–	–	60
	Kollidon® VA64	Matrix	–	–	–	–	35	–	–
	PEG 8000	Matrix	–	–	–	–	–	36	35
	croscarmellose sodium	Disintegrant	–	–	–	–	–	4	5
	PEG 1500	Plasticizer	–	–	–	–	25	–	–
Compartment3	tofacitinib	Model API	–	–	–	–	40	–	–
	Kollidon® VA 64	Matrix	–	–	–	–	35	–	–
	PEG 1500	Plasticizer	–	–	–	–	25	–	–
Shell	Eudragit® RS PO	Matrix	90	90	90	65	60	90	90
	ethyl cellulose N10	Matrix	–	–	–	15	20	–	–
	steric acid	Plasticizer	10	10	10	20	20	10	10

Table 3
Printing parameters of MED™ 3D printed design A-F tablets.

Design	Component(s)	Diameter of Nozzle (mm)	Temperature of Nozzle (℃)	Print Speed (mm/s)		Infill Density (%)	Layer Thickness (mm)
				Perimeter	Infill		
A1, A2i-iv, A3-A6	Shell	0.4	110	10	10	100	0.2
	Core	0.4	105	10	10	100	0.2
	Filler	0.4	95	10	10	100	0.2
A2v	Shell	0.3	135	25	25	100	0.2
	Core	0.4	115	15	15	100	0.18
B	Shell	0.4	110	10	10	100	0.2
	Core	0.4	114	10	10	100	0.2
	Delay layer	0.4	116	10	10	100	0.2
C	Shell	0.4	110	15	20	100	0.2
	Core	0.4	90	–	15	100	0.2
	pH-responsive layer 1 (HPMC-AS LG)	0.2	85	6.7	10	100	0.1
	pH-responsive layer 2 (HPMC-AS HG)	0.2	85	6.7	10	100	0.1
D	Shell	0.4	110	15	15	100	0.2
	Compartment 1	0.4	105	10	10	100	0.2
	Compartment 2	0.4	90	10	10	30	0.2
	Compartment 3	0.4	90	10	10	100	0.2
	Delay layer	0.4	85	10	10	100	0.2
E	Shell	0.4	120	20	20	100	0.2
	Compartment 1	0.4	100	20	20	100	0.2
	Compartment 2	0.4	70	20	20	100	0.2
	Shell	0.4	125	25	25	100	0.2
F	Compartment 1	0.8	70	25	25	100	0.2
	Compartment 2	0.6	75	25	25	100	0.2

three male beagle dogs (age: 1–1.5 years, body weight: 9–12 kg). The dogs were fasted overnight for at least 14 h prior to dosing. Each dog was then administered 150 mL fluid food intragastrically and dosed orally with a test 3D printed tablet (Design A-E). Only two beagle dogs were used for evaluation of *in vivo* pharmacokinetics of Design F tablets, with each dog received a single oral administration of a test Design F tablet in fasted states. Drinking water was available ad libitum throughout the study, and food was available at 6 h post dosing. Blood samples (~0.5 mL for each sample) were collected by venipuncture in tubes containing K_2EDTA at predetermined timepoints. The samples were immediately

Table 4
HPLC methods for the analysis of metoprolol, tofacitinib, levodopa, topiramate, and clonidine.

Model API	Column	Volume injected (μL)	Mobile phase	Flow rate (mL/min)	Detector	Column temperature(℃)
metoprolol	YMC C18 (150*4.6 mm, 5 μm)	20	0.48% ammonium acetate: ACN = 75:25	1.0	UV (275 nm)	30
levodopa	YMC C18 (150*4.6 mm, 5 μm)	20	Gradient elution: 0.01 mol/L phosphate buffer (pH 2.0): ACN = 97:3(0 ~ 3 min); 80:20 (3 ~ 7 min)	1.0	UV (280 nm)	25
tofacitinib	Agilent Eclipse Plus C18 (150* 4.6 mm, 5 μm)	20	0.02 mol/L phosphate buffer (pH 3.0): ACN = 80:20	1.0	UV (290 nm)	30
topiramate	Agilent Eclipse Plus C8 (150* 4.6 mm, 3.5 μm)	100	0.01 mol/L phosphate buffer (pH 4.0):ACN = 65:35	1.0	RID	30
clonidine	YMC Triart C18 (150*4.6 mm, 3 μm)	20	Water with 0.1% (v/v) TFA: ACN = 75:25	1.0	UV (210 nm)	40

ACN: acetonitrile; TFA: trifluoroacetic acid; UV: ultraviolet; RID: refractive index detector.

centrifuged at 4 °C, 1500 g ~ 1600 g for 10 min. Plasma was separated and transferred into new labeled tubes and placed at below −60 °C until analysis using liquid chromatography-tandem mass spectrometry (QTRAP® 5500 Mass Spectrometer, AB Sciex LLC, USA). Data are presented as mean ± standard deviation. All animal studies were conducted under an IACUC-approved animal study protocol.

2.7. Simulation of theoretical pharmacokinetic profiles

For 3D printed tablets consisting of both immediate release and zero-order extended release components, the contribution of drug release from each component to plasma concentration can be expressed using the following equations:

Immediate release:

$$C_i = \frac{F_i k_a D_i}{V(k_a - k)}\left(e^{-kt} - e^{-k_a t}\right) \tag{6}$$

Extended release:

$$C_e = \frac{k_r^0}{kV}\left(1 + \frac{k_a}{k - k_a}e^{-kt}\right) - \frac{k_r^0}{V(k - k_a)}e^{-k_a t} \tag{7}$$

where $k_r^0 = \frac{F_e \times D_e}{t_f - t_{on}}$, C_i and $C_e$represent the plasma concentration of immediate release and extended release components, respectively; $F_i$and F_e represent the bioavailability of immediate release and extended release components, respectively; $D_i$and D_e denote the dose of immediate release and extended release components, respectively; k_a and k are the absorption rate constant and elimination rate, respectively; V is the apparent distribution volume, k_r^0 is the zero-order release constant for the extended release component, t_{on} denotes the onset time for extended release, t_f is the final time for extended release, and t represents the time. The calculation of plasma concentration is based on the assumption that the model drug is absorbed and eliminated following first-order kinetics.

The total plasma concentration for the composite tablet can then be calculated as the sum of the plasma concentrations for the different components:

$$C = C_i + C_e \tag{8}$$

where C is the total apparent plasma concentration.

3. Results and discussion

3.1. MED™ 3D printing

MED™ 3D printing is developed to address the needs of producing pharmaceutical products including precision, handling multiple material, use of wide range of excipients and drugs without additional processing, large scale production, and GMP compliance. In this article, model compounds and pharmaceutical inactive ingredients in powder form were used directly for MED™ 3D printing without additional processing. The filament-free additive manufacturing process of MED™ also allows the printing of a relatively wide range of thermoplastic polymers with high drug loading (60%) that is difficult to be achieved using conventional FDM due to the inadequate mechanical properties of the prepared filaments. The GMP-compliant MED™ 3D printer provided a reliable pharmaceutical fabrication method using various excipients or combination of excipient with relatively low printing temperature. Since there is no need to prepare filament with properties that will fit the FDM printers, a wide range of selection excipients can be used to formulate the drug products. With a proper pre-formulation study, no degradation product or compatibility issues were found for the drug substances during the MED™ 3D printing process. This could be attributed to the lower printing temperature and wider selection of excipients in formulation development. With each printing station containing a single nozzle, the multiple printing stations in the MED™ 3D printer coordinated with each other to construct the specific parts of the structure (i.e., core, shell, filler, delay layer, etc.) and built a multi-component tablet with high accuracy, precision and reproducibility. As an example, in a continuous production of GMP-manufactured batch of Design B using single nozzle MED™ 3D printer with three printing stations, 347 tofacitinib citrate delayed release tablets (target weight 205.0 mg) were fabricated and an average weight of 204.9 mg with an RSD of 0.39% were obtained. The continuous feeding of powder materials and the process of MED™ 3D printing technology possess inherent advantages to creating a high throughput production line for end-to-end automated continuous manufacturing. Based on the same technology used in the R&D scale MED™ 3D printer, a GMP-compliant MED™ 3D printing system consisting of a continuous material feeding and mixing module, MED™ workstations, unloading and packaging modules, Process Analytical Technology (PAT) modules, and Supervisory Control and Data Acquisition (SCADA) module has been built. Production scaling (up to 30,000 tablets per day) has been achieved through nozzle array and can be further expanded via chaining of modularized printing head units. The integration of real-time Process Analytical Technology (PAT) and feedback control enables continuous monitoring of the manufacturing process to assure production quality, reduce manufacturing cost, and to provide convenience for regulatory audit. Many desirable features for modern pharmaceutical production are also incorporated to make the MED™ 3D printing system to be compact, modular, capable of continuous manufacturing, scalable, flexible, and intelligent. The system allows modified release drug tablet products to be manufactured efficiently at any desired scales, presenting a promising direction of the next generation pharmaceutical manufacturing.

3.2. Designs for modulation of release rates

Utilizing the compartment model, Design A (varying surface area and layer height) with metoprolol in the compartment (Fig. 8a), a range of metoprolol release profiles were achieved. The Eudragit RS®-based shell remains intact throughout the metoprolol release process, whereas the HPC-based drug core dissolves layer-by-layer via a surface erosion mechanism. As summarized in Table 5, the metoprolol content measured from the *in vitro* dissolution studies agreed well with the theoretical metoprolol content (100 mg) of the Design A tablets, confirming that no significant drug loss occurred during the printing process. Tablet Design A1 produced an *in vitro* metoprolol release profile that followed zero-order release kinetics (Fig. 8b), since the surface area remained constant for each core layer. The dissolution rate (R_D) of drug-containing matrix (0.25 mm/h) was determined from the slope of metoprolol release profile. The dissolution rate and the height of the metoprolol-containing compartment were used to generate the theoretical release profiles for the remaining Design A tablet series that consisted of various drug compartment shapes. Although about 7% more metoprolol was released from the A1 tablet design within the first hour of dissolution as compared with the theoretical predictions, the rate of release is consistent with the theoretical simulation and the entire dissolution curve was shifted slightly upward after the first hour as well as for some of the other designs (Fig. 8a). The shift was probably due to slight swelling of the matrix polymer upon contact with water, and further improvement of the design is ongoing to address the issue of increased release in the first hour that deviated from the theoretical predictions.

Using the release profile of A6 as an example (Fig. 8c) for variable rate release, the tablets designed with stepwise changes in surface area exhibited a stepwise change in release rate corresponding to the surface area of the multilayered drug in the compartment. Predicted drug release characteristics based on the shape and surface area of the multilayer compartment, such as stepwise decreasing (A2i-iv), continuous decreasing (A3), stepwise increasing (A4), increasing–decreasing (A5), and decreasing-increasing (A6) release rates were successfully demonstrated. The release rate for each metoprolol-containing layer within the drug compartment is summarized in Table 5. The relationship between the surface area of the exposed layer from which metoprolol can be released and the actual metoprolol release rate is depicted in Fig. 8d. A linear relationship (slope = 0.3214, $R^2 = 0.9832$) was noted, indicating that the metoprolol release rate was directly proportional to the surface area of the exposed layer from which metoprolol can be released. Therefore, the release rate or amount at a given time point or over a time interval can be controlled by altering the surface area for drug release in the delivery system. The similarity factor *f2* (Table 5) demonstrated the agreement between the experimental and simulated metoprolol release profiles for Design A tablets. All of the *f2* values obtained were above 54 for each of the Design A formulations. The agreement observed between the theoretical calculations and the experimental results provides a foundation for the formulation by design process that will be discussed in Section 3.5.

Readily modulating release rates in a predictable manner can be an effective tool for generating a desired drug release profile for efficient product development and can be of significant interest for clinical application. Creating formulations with a constant release rate is clinically desirable in maintaining a stable plasma concentration during treatment. A predictably decreasing release rate profile could be useful when a large initial dose of drug is required to relieve the symptom, such as pain, followed by a decreasing dose to maintain the therapeutic effect. Development of an increasing release rate profile could be important for maintaining a desired plasma concentration for drugs that exhibit a reduced rate of absorption as the dosage form moves along the GI tract. A few technologies, such as Geomatrix®, have been used to successfully develop drug products exhibiting zero-order release [26] and biphasic release (quick-slow and slow-quick) profiles. However, it remains a

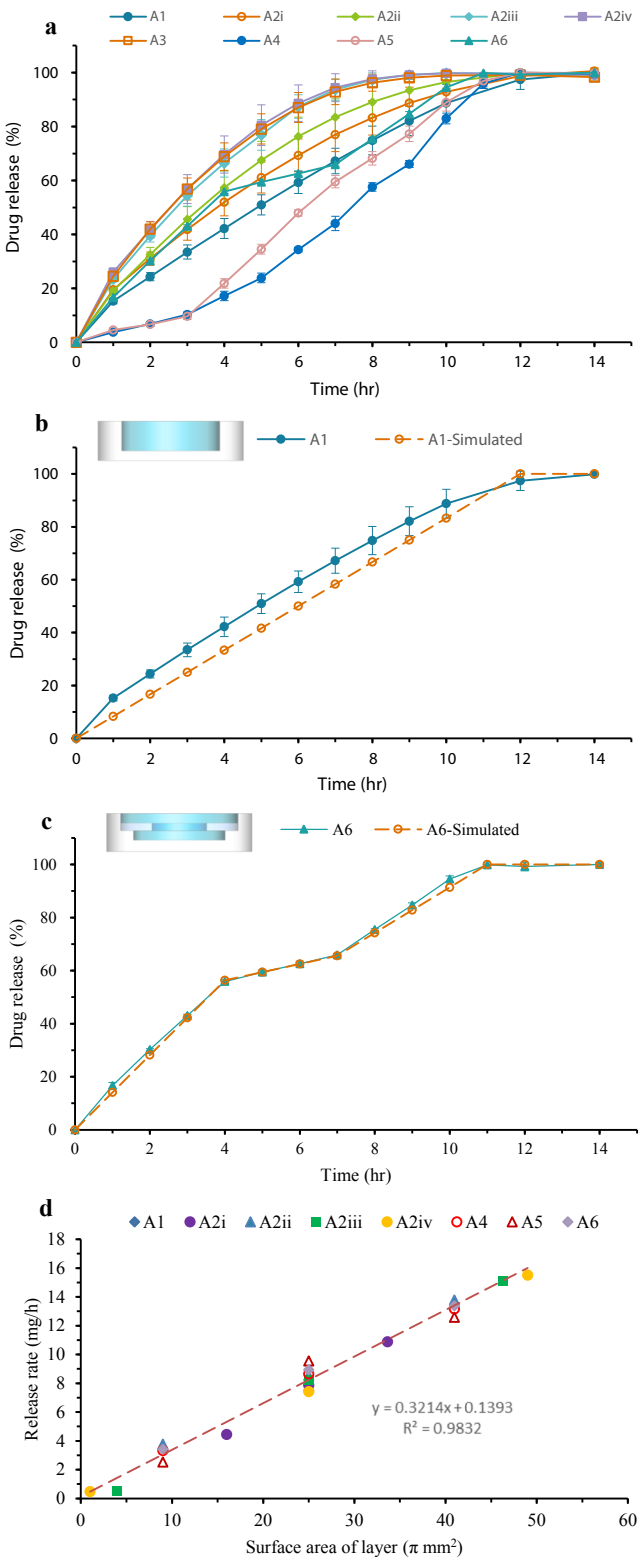

Fig. 8. Metoprolol release profiles of Design A tablets designed with various drug compartment shapes. (a) Experimental metoprolol release profiles of 3D printed A1-A6 tablets. (b) Simulated and experimental metoprolol release profiles of the 3D printed A1 tablets. (c) Simulated and experimental metoprolol release profiles of the 3D printed A6 tablets. (d) Relationship between the designed surface area from which metoprolol can be released and the metoprolol release rate. Data are presented as mean ± SD (n = 6).

Table 5
Surface areas and metoprolol release rates of each layer within the multilayered drug compartment in Design A tablets. Data are presented as mean ± SD (n = 6).

Design		Surface area (mm^2)	Release rate (mg/h)	Tablet metoprolol content (mg)	Similarity factor (*f2*)
A1	Column	25π	7.5 ± 0.3 *	98.10 ± 1.25	58
A2i	Layer 1	33.64π	10.9 ± 0.2 *	100.78 ± 0.90	60
	Layer 2	25π	7.9 ± 0.3		
	Layer 3	16π	4.5 ± 0.4		
A2ii	Layer 1	40.96π	13.8 ± 0.3 *	100.17 ± 2.23	70
	Layer 2	25π	8.5 ± 0.6		
	Layer 3	9π	2.8 ± 0.5		
A2iii	Layer 1	46.24π	15.1 ± 0.7 *	102.55 ± 1.47	59
	Layer 2	25π	8.2 ± 0.9		
	Layer 3	4π	0.5 ± 0.3		
A2iv	Layer 1	49π	15.5 ± 0.5 *	101.22 ± 1.74	61
	Layer 2	25π	7.4 ± 0.9		
	Layer 3	π	0.5 ± 0.3		
A3	Top	56.25π	–	101.95 ± 0.70	54
	Bottom	4π	–		
A4	Layer 1	9π	3.3 ± 0.1 *	101.62 ± 0.46	90
	Layer 2	25π	8.6 ± 0.5		
	Layer 3	40.96π	13.2 ± 0.7		
A5	Layer 1	9π	2.5 ± 0.3 *	100.05 ± 0.28	76
	Layer 2	40.96π	12.6 ± 0.2		
	Layer 3	25π	9.6 ± 0.3		
A6	Layer 1	40.96π	13.4 ± 0.1 *	102.47 ± 0.45	94
	Layer 2	9π	3.4 ± 0.1		
	Layer 3	25π	8.9 ± 0.5		

* Linear portion of the data (after 1 h) was taken for regression.

challenging task for any single technology to reliably produce a formulation with all types of release profiles in a predictable manner. 3D printing technology offers new opportunities for developing drug delivery systems with a wide variety of release profiles, including release profiles not currently possible with existing technologies. For example, Tagami et al. used a modified dual-nozzle FDM 3D printer to develop PVA-PLA composite tablets with varying drug release rates [27]. However, authors encountered challenge in developing composite tablets with increasing release rates due to the insufficient exposure of drug component to release medium. When constructed with multiple printing stations using a multilayered drug compartment design, MED™ 3D printer was able to handle multiple materials by incorporating water soluble fillers to confine the drug layers within a designed space. Dissolution of the fillers occurs at the same rate as the drug layer, ensuring complete exposure of the subsequent drug layers to the dissolution medium. As demonstrated in other designs, tablet dosage forms with other types of release profiles, including zero-order release, decreasing release, increasing–decreasing release, and decreasing-increasing release can be fabricated with excellent reproducibility in a single step process based on the multilayered compartment design and MED™ 3D printing technology.

3.3. Designs for control of onset time and release sites

3D Printed Design B tablets (modified release with delayed onset time) containing tofacitinib were fabricated with or without a layer to seal the drug containing core. *In vitro* release profiles of Design B tablets with and without a delay layer are shown in Fig. 9c. The amount of tofacitinib released from Design B tablets with a delay layer of 0 mm, 0.2 mm, and 0.4 mm thickness was 10.87 ± 0.28 mg, 11.18 ± 0.15 mg, and 11.65 ± 0.11 mg, respectively, all of which agreed well with the theoretical drug content (11 mg), indicating that no significant drug loss occurred during the printing process. The control tablets without a delay layer exhibited no delay in tofacitinib release, while the onset of tofacitinib release was delayed upon the addition of thicker delayed release layers. The delayed onset time was linearly proportional to the layer thickness as depicted in Fig. 9d. A delay layer thickness of 0.2 mm or 0.4 mm resulted in an *in vitro* onset time of 1.5 h and 3 h, respectively. When the zero order release drug core was fabricated in conjunction with the delay layer, the onset time shifted accordingly while the *in vitro* zero order release profile remained the same. Compared to the control tablets (T_{max} = 2.00 ± 0 h), the T_{max} of tablets with a 0.2 mm delay layer was delayed by 1.33 ± 0.47 h (Fig. 9e), congruent with the 1.5-hour lag time

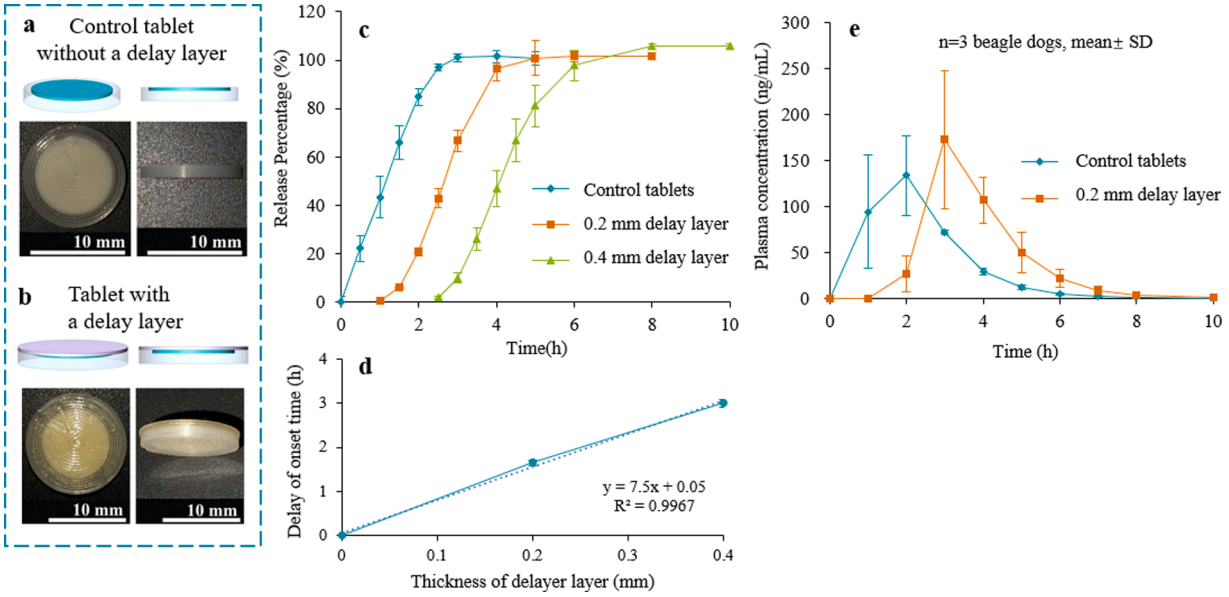

Fig. 9. *In vitro* and *in vivo* studies of MED™ 3D printed Design B tofacitinib tablets. Printed tofacitinib tablets without a delay layer (a) and with a delay layer (b): shell (transparent), drug core (white), delay layer (transparent yellow). (c) Release profiles of tofacitinib tablets with a delay layer with increasing layer thickness (0 mm, 0.2 mm, 0.4 mm). Data are presented as mean ± SD (n = 6). (d) Relationship between thickness of the delay layer and delayed onset of release *in vitro*. Data are presented as mean ± SD (n = 6). (e) Tofacitinib plasma concentration–time profiles in healthy beagle dogs after oral administration of control tablets and tablets with 0.2 mm delay layer. Data are presented as mean ± SD (n = 3).

observed *in vitro*. The results from this design show the independency of each component in the 3D printed tablet and reinforce the predictability and reproducibility of this approach.

Design C tablets containing metoprolol were fabricated with or without a pH-responsive layer to release metoprolol at a desired intestinal region after passing through the stomach. Fig. 10 depicts the mean percentages of metoprolol released from these tablets *in vitro*. The percentage of metoprolol recovered from the drug release study was found to be 99.6 ± 0.4%, 101.1 ± 1.0%, 98.4 ± 1.3%, respectively, indicating that no significant drug loss occurred during the printing process. Tablets without a pH-responsive layer released more than 90% of metoprolol within 15 min at gastric pH. For tablets sealed with an HPMC-AS LG layer, no metoprolol was detected in the acidic dissolution medium for the first two hours. The release of metoprolol was only triggered after being placed in pH 5.8 phosphate buffer and release was then complete in 45–60 min. Tablets sealed with an HPMC-AS HG layer exhibited a similar release behavior after being exposed to the pH 6.8 dissolution medium after total of 4 h exposure to pH 1.2 and pH 5.8, although about 3% and 7% of metoprolol prematurely released in pH 1.2 and pH 5.8 dissolution media, respectively. These results demonstrated that by employing different pH-responsive layers, the enteric sealing layer can prevent the release of drug in the stomach and delay release until reaching the duodenum (pH 5.8) or jejunum (pH 6.8) [28], whereas omitting the sealing layer allows release of drug in the stomach. A thickness of 0.1 mm or less of enteric sealing layer was deemed critical to trigger the release of drug immediately after being exposed to buffer solutions mimicking intestinal pH conditions. The structure of the core also plays a role in drug release. A fully filled core structure exhibited slower metoprolol release rates than a structure with a zig-zag pattern. The slower release rate could be attributed to the gelation of Kollidon VA 64 matrix and insufficient contact with the release medium.

Modulating onset time has clinical significance. Releasing the drug at the right time can optimize therapeutic outcomes. For example, circadian rhythm related diseases such as rheumatoid arthritis [29], hypertension [30], cardiac arrhythmia [31], and nocturnal asthma [32] often are optimally treated with a drug onset time that is not convenient for patients to take the medication. Taking a medication at a convenient time and having its therapeutic action reach maximal effect at the optimum time of day can improve or optimize therapeutic outcomes. 3D printed tablets with a well-controlled onset time, as demonstrated in this study, can provide a platform to address the clinical needs for delayed release formulations.

Another therapeutic option to optimize therapy is the development of site-specific drug delivery systems that deliver drugs to specific locations in the gastrointestinal tract to maximize plasma concentrations by, for example, releasing drug in the stomach or small intestine if optimal absorption occurs at one location versus another (i.e., absorption is favored in a more acidic environment or a more basic environment). For drugs that can be or should be absorbed in a specific region of small intestine, controlled release of drug can also be achieved by utilizing the difference in pH along the gastrointestinal tract to release the drug in a specific location to maximize the therapeutic benefits and reduce side effects [33]. To date, examples of well controlled release for GI site-specific delivery fabricated by 3D printing have been limited. A few previous studies have reported the use of FDM 3D printing technology to fabricate site-specific drug delivery systems that release drugs in a specified region of GI tract after passing through the stomach [34,35], or to prototype delayed release solid dosage forms with an erodible shell or layer or control off-release periods of the drug core by changing thickness of the erodible component [15,22]. The latter methods, however, used a complicated process that required an additional step to incorporate the drug formulation in different forms into the printed polymeric shell. When combined with multiple compartment designs, the same drug or multiple drugs in single tablet for delivery in different GI location can be developed and fabricated using MED™ 3D printing process with a predictable and reproducible result.

3.4. Combination of APIs and release kinetics

In additon to single compartment structure tablets, multiple compartments in a single tablet can easily be designed and fabricated using MED™ 3D printing technology. A tablet composed of two drugs was designed to contain multiple compartments to achieve drug release with different release kinetics. Since each compartment can be designed to provide independent release kinetics, it simplifies formulation development and allows for fine-tuning of the release parameters for one of the drugs without affecting the release characteristics of other drug. Based on this design concept, a three-compartment model (Fig. 4) was used to provide the release of one of the two drugs via zero order release kinetics and the other drug via pulsatile release. The pulsatile release was achieved by creating an immediate release and a delayed release of the drug from two independent compartments.

In vitro drug release profiles of MED™ 3D printed multi-compartment tablets, containing metoprolol and tofacitinib are shown in Fig. 11b. The amount of tofacitinib and metoprolol released from Design D tablets was 10.90 ± 0.40 mg and 25.22 ± 0.17 mg, respectively, all of which agreed well with the theoretical drug content (11 mg and 25 mg), indicating that no significant drug loss occurred during the

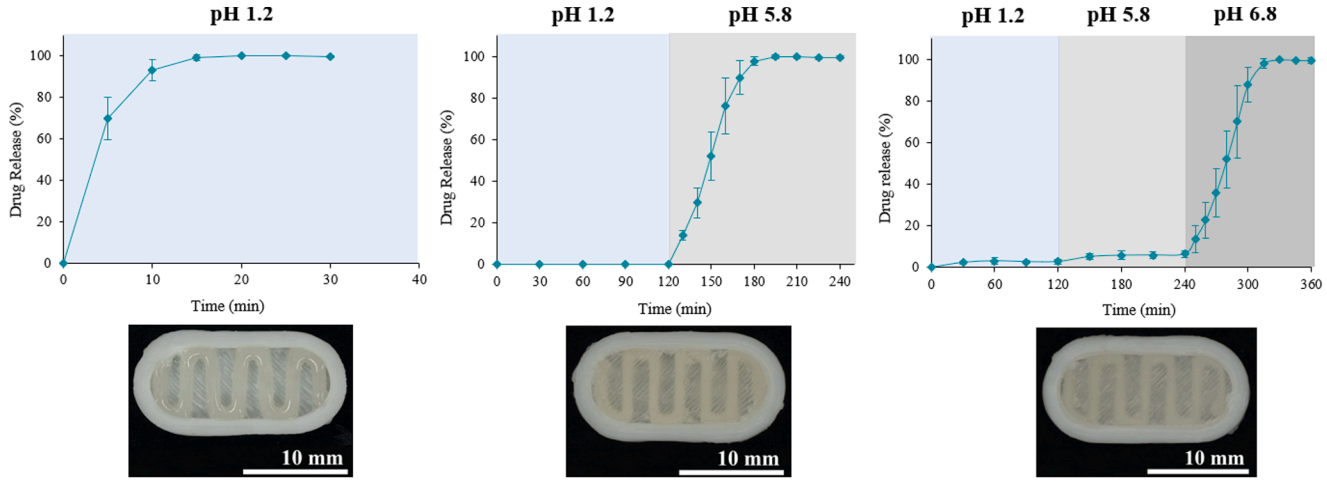

a. Tablet without a pH-responsive layer **b**. Tablet with a 0.1mm HPMC-AS LG layer **c**. Tablet with a 0.1mm HPMC-AS HG layer

Fig. 10. *In vitro* release of MED™ 3D printed Design C tablets. Drug release profiles (top) and appearance (bottom) of (a) tablets without pH-responsive layer, (b) tablets with an HPMC-AS LG layer responding to pH 5.8, (c) tablets with an HPMC-AS HG layer responding to pH 6.8. Data are presented as mean ± SD (n = 3).

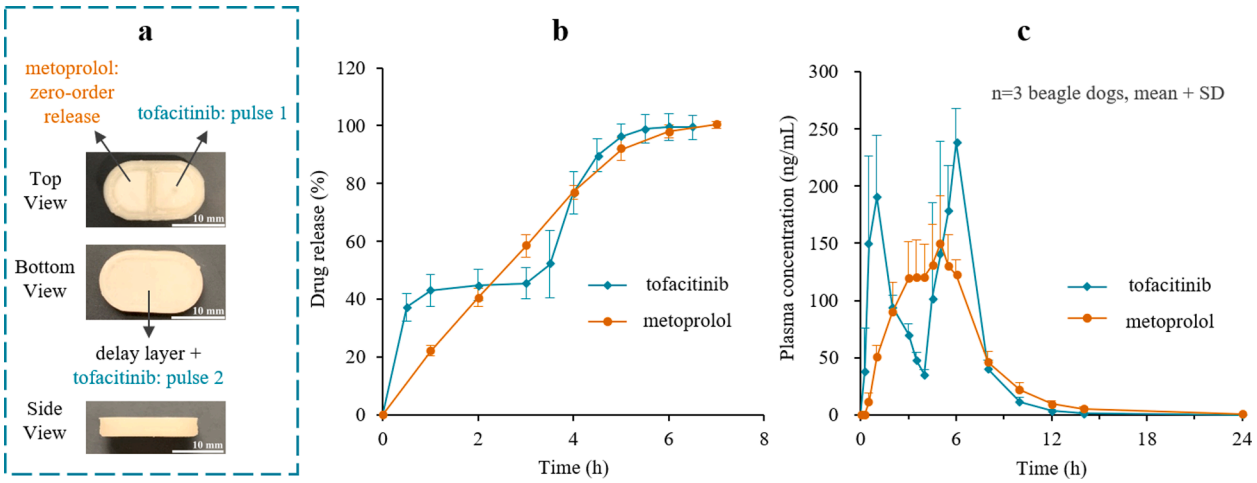

Fig. 11. *In vitro* and *in vivo* studies of MED™ 3D printed Design D tablets containing both metoprolol and tofacitinib. (a) 3-compartment fixed-dose combination tablets: shell (pale white), drug core (pale yellow), delay layer (pale yellow). (b) Drug release profiles of the printed fixed-dose combination tablets in pH 6.8 phosphate buffer: tofacitinib (teal), metoprolol (orange). Data are presented as mean ± SD (n = 6). (c) Metoprolol and tofacitinib plasma concentration–time profiles in healthy beagle dogs after oral administration of MED™ 3D printed fixed-dose combination tablets (n = 3), tofacitinib (teal), metoprolol (orange). Data are presented as mean + SD (n = 3).

printing process. Tofacitinib exhibited an immediate release of about 43% of the total dose within the first hour and then a second release of the remaining 57% of dose at the fourth hour. Independently, the metoprolol component exhibited a six-hour zero-order release kinetic profile. An *in vivo* study in beagle dogs also clearly demonstrated a pharmacokinetic profile of a sustained release plasma level of metoprolol within the period of 6 h and two-pulse release for tofacitinib with peak plasma level at 1-hour and 6-hours, respectively (Fig. 11c).

Application of multiple compartment or multiple formulation design can also be used to modulate the release kinetics of a drug by combining both immediate release (IR) and extended release (ER) characteristics of the same drug in a single tablet (Design E). Using the pharmacokinetics data obtained separately from immediate release and extended release formulations, the pharmacokinetic profile of a combination of immediate release and extended release can be simulated. The target pharmacokinetic profile can be obtained by varying the ratio of immediate release and extended release components according to the targeted blood concentration. A two-compartment tablet was fabricated with one compartment containing levodopa immediate release formulation and the other compartment containing levodopa extended release formulation. Based on the pharmacokinetic profiles (Fig. 12b) of 3D printed IR and ER tablets of levodopa, a simulation of pharmacokinetics was performed using the method described in section 2.7 using varying IR to ER ratios. The simulation result is shown in Fig. 12c. Based on the simulation results, a 1:1 levodopa IR to ER component ratio would provide the target pharmacokinetic profile. After fabrication of Design E tablets with

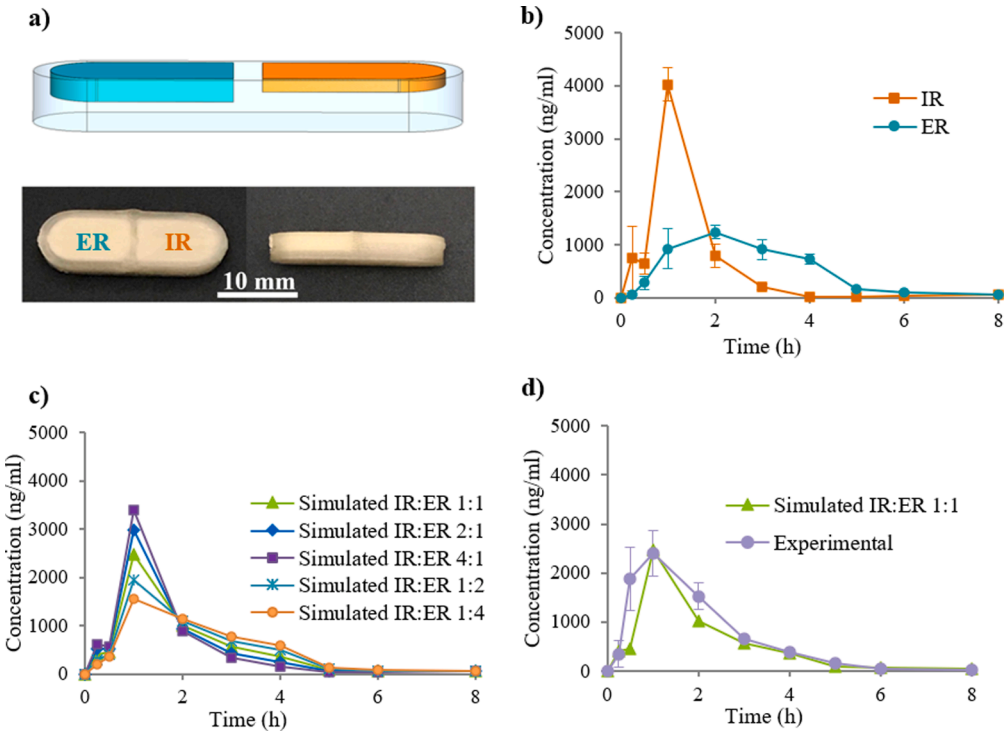

Fig. 12. *In vivo* pharmacokinetic studies of 3D printed IR, ER, and combination tablets (Design E) containing levodopa. (a) Multi-compartment design that combines IR (orange) and ER (teal) components in separate compartments in a single tablet (top), and the appearance of the printed tablets. (b) Levodopa plasma concentration–time profiles in fed healthy beagle dogs after oral administration of IR or ER tablets. (c) Simulated levodopa plasma concentration–time profiles with variable ratios of IR and ER components combined. (d) Levodopa plasma concentration–time profile (lavender) in healthy beagle dogs after oral administration of the Design E tablet (IR: ER = 1:1) and the simulated profile (green). Data are presented as mean ± SD (n = 3).

1:1 immediate release and extended release in two separate compartments, the prediction that a 1:1 IR to ER ratio would provide the target pharmacokinetic profile was verified in an *in vivo* study by oral administration of 3D printed tablets to beagle dogs fed with low-fat diet (Fig. 12d).

In addition to two-compartment designs, the layering design of two formulations in single compartment can also be used to modulate the *in vivo* pharmacokinetic profile by sequential release of drug from one compartment. As shown in Fig. 13, sequentially layering IR and ER components in Design F tablet can also provide a fine-tuned pharmacokinetic profile for topiramate with an IR: ER ratio of 1:7 for a desired pharmacokinetic profile.

These two examples of modulating pharmacokinetic profiles can be of practical significance in pharmaceutical product development. This approach allows formulation scientists to develop a formulation analogous to snapping Legos with different release characteristics together to obtain a desired *in vivo* profile, which can aid early-stage formulation development and avoid the drawback of compounds with a less than ideal half-life. Additionally, it can be used for post-marketing efforts in life cycle management of approved drugs by developing once-daily products. Such an innovative "Lego Building" design approach can also be used efficiently to assembly a tablet with multiple drugs and release kinetics in a single 3D printed tablet.

3.5. 3D printing formulation by design (3DPFbD®) approach

Current pharmaceutical formulation development still heavily relies on the traditional trial-and-error methods, which is time consuming and also brings uncertainty to the development process. Because of the lengthy and complex process of drug development as well as the cost incurred to bring a drug to market, any technology that can accelerate the product development timeline will benefit both patients and the pharmaceutical industry. The predictability and reproducibility of drug delivery systems created using MED™ 3D printing technology as shown in the examples of this study form the basis for a 3D printing formulation by design (3DPFbD®) approach. A general workflow for 3DPFbD® is shown in Fig. 14.

Using Design A2v as an example, when a desired release profile (Fig. 15a) is defined based on the proposed *in vitro* release profile and pharmacokinetics, a multilayered compartment design (Fig. 15b) that can achieve the target profile is selected from the model database. Based on the selected tablet design, the excipients used to construct different components of the designed structure (core and shell, Table 2) are chosen from the material database. By dividing the target release profile into multiple time segments with each segment corresponding to a designed layer in the multilayered drug compartment, the thickness and the surface area of each drug layer was determined based on matrix dissolution rate (R_D), release duration, drug loading percentage in the matrix, and the matrix density. The designed tablets are rapidly prototyped using a MED™ 3D printer followed by characterization *in vitro* and/or *in vivo*. The experimental results are then compared with the target release profiles to determine if minor calibration of structure parameters, material parameters, or formulation parameters is necessary. As depicted in Fig. 15c, the drug release profile of 3D printed tablet with multilayered drug compartment agreed well with the target release profile ($f2 = 75$), and the amount of clonidine released from Design A2v tablets (101.5 ± 2.0 μg) agreed well with the theoretical drug content (100 μg). The results from developing Design A2v tablet demonstrated that 3DPFbD® is a predictable and reliable approach to circumvent the traditional trial and error method in formulation development, which can lead to a change of the current practice in product development.

In summary, this study demonstrated that MED™ 3D printing technology and printers developed based on this technology can meet the pharmaceutical needs in precision, reproducibility, and GMP requirements. Tablets with various release characteristics can be fabricated using MED™ 3D printer to provide desired *in vitro* and *in vivo* profiles for different product development and clinical applications in an efficient and predictable manner.

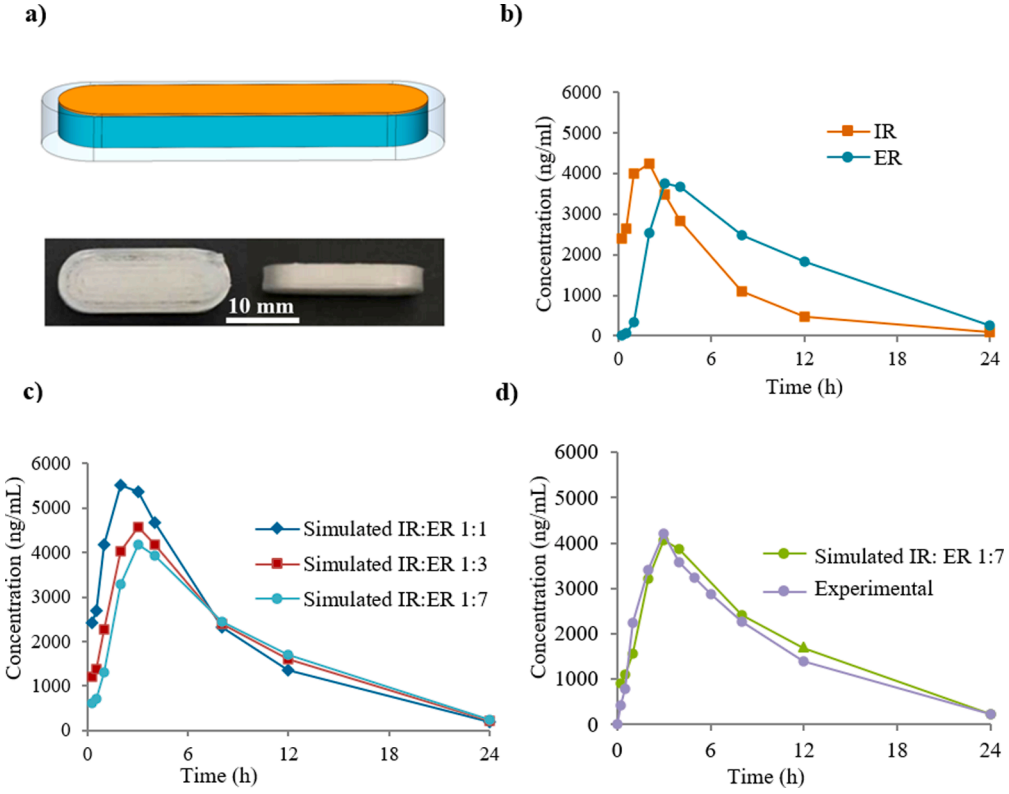

Fig. 13. *In vivo* pharmacokinetic studies of 3D printed IR, ER, and dual release mode tablets (Design F) containing topiramate. (a) Single compartment design that combines IR (orange) and ER (teal) components by sequential layering (top), and the printed tablets (bottom). (b) Topiramate plasma concentration–time profiles in fasted healthy beagle dogs after oral administration of IR or ER tablets. (c) Simulated topiramate plasma concentration–time profiles with variable ratios of IR and ER components combined. (d) Topiramate plasma concentration–time profile (lavender) in healthy beagle dogs after oral administration of the Design F tablet (IR: ER = 1:7) and the simulated profile (green). Data are presented as mean (n = 2).

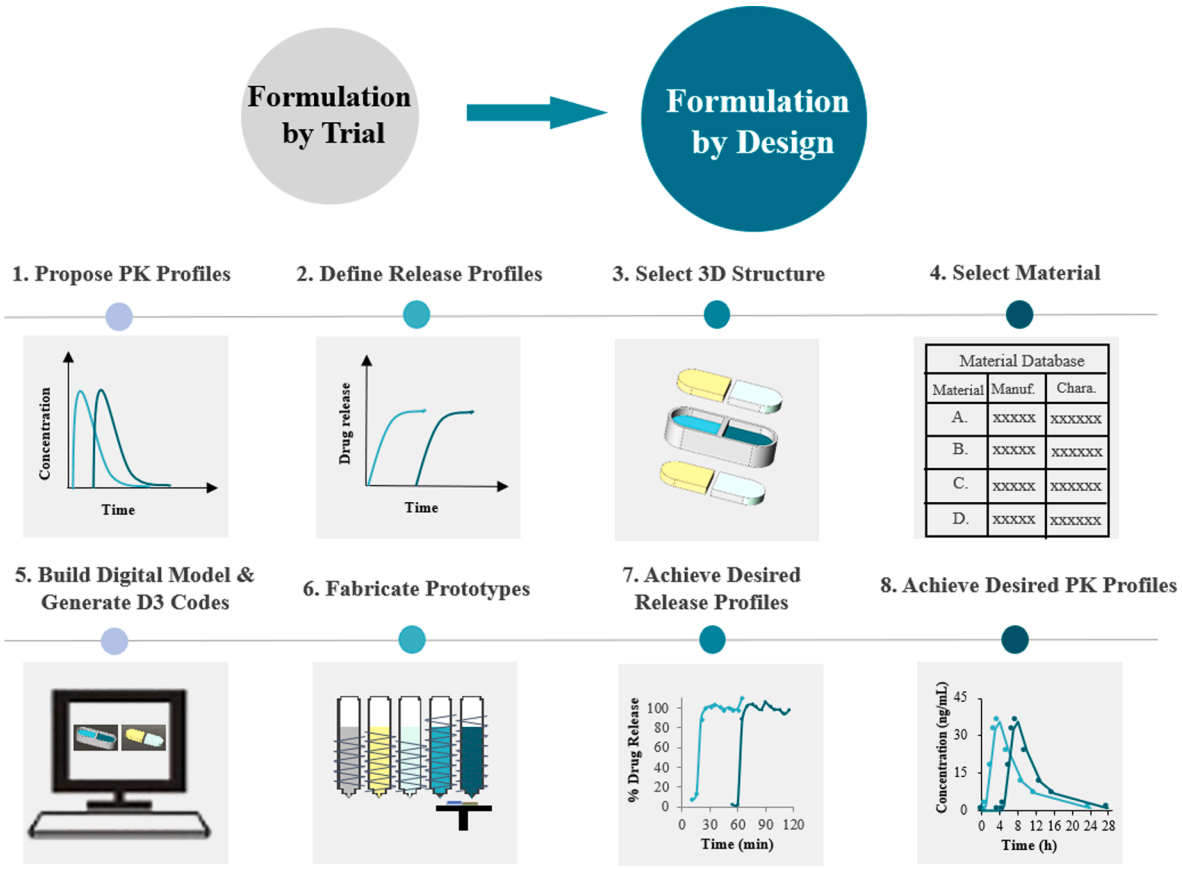

Fig. 14. Schematic Diagram of 3D Printing Formulation by design (3DPFbD®) Approach.

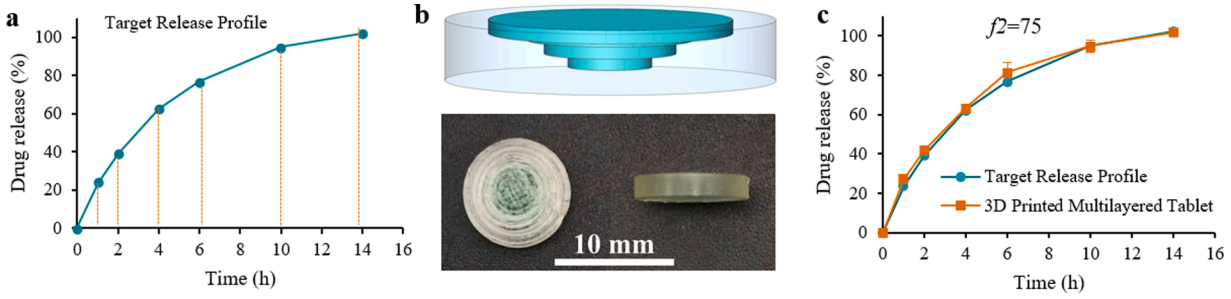

Fig. 15. Application of 3D Printing Formulation by design (3DPFbD®) to formulate 3D printed tablet (Design A2v) containing clonidine to achieve target release profile. (a) Target release profile (teal) of clonidine. (b) Top: 3D design of clonidine tablet with multilayered drug compartment. Bottom: rapid prototyped clonidine tablet with multilayered drug compartment. Shell (pale white), drug core (teal). (c) Experimental release profile (orange) of clonidine from MED™ 3D printed tablets. Data are presented as mean ± SD (n = 6).

4. Conclusion

A novel MED™ 3D printing technology has been developed to circumvent several drawbacks of fused deposition modeling (FDM) including the requirement for pre-fabrication of printable drug-loaded filament and printing precision. The MED™ technology uses active ingredient and excipient materials in powder form as starting materials without the filament formulation burden as in FDM 3D printing. The high throughput printer nozzle array, handling multiple materials, and precision control of deposition in MED™ 3D printing make the reproducibility, accuracy and mass production of 3D printing pharmaceutical manufacturing possible.

Design and fabrication of 3D printed tablets using compartmental models provides reliable solutions for controlling the release onset time, duration, kinetics and mode for different clinical and product development needs. The predictability of release behavior of MED™ 3D printed tablet form the foundation for the 3D printing formulation by design (3DPFbD®) approach and provides an efficient and reliable tool for pharmaceutical product development . The application of MED™ 3D printing technology in pharmaceutical areas could lead to a paradigm shift in controlled drug delivery and pharmaceutical product development.

CRediT authorship contribution statement

Yu Zheng: Methodology, Investigation, Formal analysis, Writing - original draft, Writing - review & editing, Project administration. **Feihuang Deng:** Methodology, Project administration. **Bo Wang:** Investigation. **Yue Wu:** Investigation. **Qing Luo:** Investigation. **Xianghao Zuo:** Investigation, Validation. **Xin Liu:** Data curation. **Lihua Cao:** Resources,

Formal analysis. **Min Li:** Investigation. **Haohui Lu:** Resources. **Senping Cheng:** Funding acquisition, Supervision. **Xiaoling Li:** Conceptualization, Writing - review & editing, Supervision.

Declaration of Competing Interest

All work was performed in Triastek, Inc. Authors have applied the following patents:

1) PCT patent application WO2018210183. 2018 Nov 5.
2) PCT patent application WO2019137199. 2018 Dec 25.
3) PCT patent application WO2018137686. 2018 Jan 25.
4) PCT patent application WO2016192680. 2016 March 6.
5) PCT patent application WO2019137333. 2019 July 1.

References

[1] Awad, A., Fina, F., Trenfield, S.J., Patel, P., Goyanes, A., Gaisford, S., Basit, A.W., 2019. 3D printed pellets (miniprintlets): a novel, multi-drug, controlled release platform technology. Pharmaceutics 11 (4).

[2] Goyanes, A., Madla, C.M., Umerji, A., Duran Pineiro, G., Giraldez Montero, J.M., Lamas Diaz, M.J., Gonzalez Barcia, M., Taherali, F., Sanchez-Pintos, P., Couce, M. L., Gaisford, S., Basit, A.W., 2019. Automated therapy preparation of isoleucine formulations using 3D printing for the treatment of MSUD: First single-centre, prospective, crossover study in patients. Int. J. Pharm. 567, 118497.

[3] Wu, B.M., Borland, S.W., Giordano, R.A., Cima, L.G., Sachs, E.M., Cima, M.J., 1996. Solid free-form fabrication of drug delivery devices. J. Control. Release 40 (1–2), 77–87.

[4] Katstra, W.E., Palazzolo, R.D., Rowe, C.W., Giritlioglu, B., Teung, P., Cima, M.J., 2000. Oral dosage forms fabricated by three dimensional printing. J Control Release 66 (1), 1–9.

[5] Kyobula, M., Adedeji, A., Alexander, M.R., Saleh, E., Wildman, R., Ashcroft, I., Gellert, P.R., Roberts, C.J., 2017. 3D inkjet printing of tablets exploiting bespoke complex geometries for controlled and tuneable drug release. J. Control Release 261, 207–215.

[6] Isreb, A., Baj, K., Wojsz, M., Isreb, M., Peak, M., Alhnan, M.A., 2019. 3D printed oral theophylline doses with innovative 'radiator-like' design: Impact of polyethylene oxide (PEO) molecular weight. Int J Pharm 564, 98–105.

[7] Goyanes, A., Buanz, A.B., Hatton, G.B., Gaisford, S., Basit, A.W., 2015. 3D printing of modified-release aminosalicylate (4-ASA and 5-ASA) tablets. Eur. J. Pharm. Biopharm. 89, 157–162.

[8] Fina, F., A. Goyanes, M. Rowland, S. Gaisford, and W.B. A, 3D Printing of Tunable Zero-Order Release Printlets. Polymers (Basel), 2020. 12(8).

[9] Sadia, M., Arafat, B., Ahmed, W., Forbes, R.T., Alhnan, M.A., 2018. Channelled tablets: An innovative approach to accelerating drug release from 3D printed tablets. J. Control Release 269, 355–363.

[10] Martinez, P.R., Goyanes, A., Basit, A.W., Gaisford, S., 2017. Fabrication of drug-loaded hydrogels with stereolithographic 3D printing. Int. J. Pharm. 532 (1), 313–317.

[11] Li, P., Zhang, S., Sun, W., Cui, M., Wen, H., Li, Q., Pan, W., Yang, X., 2019. Flexibility of 3D extruded printing for a novel controlled-release puerarin gastric floating tablet: design of internal structure. AAPS PharmSciTech 20 (6), 236.

[12] Trenfield, S.J., Tan, H.X., Goyanes, A., Wilsdon, D., Rowland, M., Gaisford, S., Basit, A.W., 2020. Non-destructive dose verification of two drugs within 3D printed polyprintlets. Int. J. Pharm. 577, 119066.

[13] Khaled, S.A., Alexander, M.R., Wildman, R.D., Wallace, M.J., Sharpe, S., Yoo, J., Roberts, C.J., 2018. 3D extrusion printing of high drug loading immediate release paracetamol tablets. Int. J. Pharm. 538 (1–2), 223–230.

[14] Fina, F., Goyanes, A., Madla, C.M., Awad, A., Trenfield, S.J., Kuek, J.M., Patel, P., Gaisford, S., Basit, A.W., 2018. 3D printing of drug-loaded gyroid lattices using selective laser sintering. Int. J. Pharm. 547 (1–2), 44–52.

[15] Smith, D., Kapoor, Y., Hermans, A., Nofsinger, R., Kesisoglou, F., Gustafson, T.P., Procopio, A., 2018. 3D printed capsules for quantitative regional absorption studies in the GI tract. Int. J. Pharm. 550 (1–2), 418–428.

[16] Okwuosa, T.C., Pereira, B.C., Arafat, B., Cieszynska, M., Isreb, A., Alhnan, M.A., 2017. Fabricating a shell-core delayed release tablet using dual FDM 3D printing for patient-centred therapy. Pharm. Res. 34 (2), 427–437.

[17] Genina, N., Boetker, J.P., Colombo, S., Harmankaya, N., Rantanen, J., Bohr, A., 2017. Anti-tuberculosis drug combination for controlled oral delivery using 3D printed compartmental dosage forms: from drug product design to in vivo testing. J. Control. Release 268, 40–48.

[18] Khaled, S.A., Burley, J.C., Alexander, M.R., Yang, J., Roberts, C.J., 2015. 3D printing of tablets containing multiple drugs with defined release profiles. Int. J. Pharm. 494 (2), 643–650.

[19] Haring, A.P., Tong, Y., Halper, J., Johnson, B.N., 2018. Programming of multicomponent temporal release profiles in 3D printed polypills via core-shell, multilayer, and gradient concentration profiles. Adv. Healthc Mater. 7 (16), e1800213.

[20] Senping Cheng, X.L., Feihuang Deng, Haohui Lu, Haili Liu, Juan Yao, Xiaofei Wang, Wei Wu, 3D printing device and method. 2018.

[21] Goyanes, A., Allahham, N., Trenfield, S.J., Stoyanov, E., Gaisford, S., Basit, A.W., 2019. Direct powder extrusion 3D printing: Fabrication of drug products using a novel single-step process. Int. J. Pharm. 567, 118471.

[22] Tan, Y.J.N., Yong, W.P., Kochhar, J.S., Khanolkar, J., Yao, X., Sun, Y., Ao, C.K., Soh, S., 2020. On-demand fully customizable drug tablets via 3D printing technology for personalized medicine. J. Control Release 322, 42–52.

[23] Pereira, B.C., Isreb, A., Isreb, M., Forbes, R.T., Oga, E.F., Alhnan, M.A., 2020. Additive manufacturing of a point-of-care "Polypill:" fabrication of concept capsules of complex geometry with bespoke release against cardiovascular disease. Adv. Healthc Mater. 9 (13), e2000236.

[24] DACHTLER, M., HUBER, G., Polyvalent dosage forms and method for their production. 2020.

[25] Tsong, Y., Sathe, P.M., Shah, V.P., 2003. In vitro dissolution profile comparison. Encyclopedia of Biopharmaceutical Statistics, Second Edition, Marcel Dekker, Inc., New York, 2003: p. 456J462.

[26] Moodley, K., Pillay, V., Choonara, Y.E., du Toit, L.C., Ndesendo, V.M., Kumar, P., Cooppan, S., Bawa, P., 2012. Oral drug delivery systems comprising altered geometric configurations for controlled drug delivery. Int. J. Mol. Sci. 13 (1), 18–43.

[27] Tagami, T., Nagata, N., Hayashi, N., Ogawa, E., Fukushige, K., Sakai, N., Ozeki, T., 2018. Defined drug release from 3D-printed composite tablets consisting of drug-loaded polyvinylalcohol and a water-soluble or water-insoluble polymer filler. Int. J. Pharm. 543 (1–2), 361–367.

[28] Hatton, G.B., Yadav, V., Basit, A.W., Merchant, H.A., 2015. Animal farm: considerations in animal gastrointestinal physiology and relevance to drug delivery in humans. J. Pharm. Sci. 104 (9), 2747–2776.

[29] Cutolo, M., 2016. Glucocorticoids and chronotherapy in rheumatoid arthritis. RMD Open 2 (1), e000203.

[30] Mathur, P., Kadavath, S., Marsh, J.D., Mehta, J.L., 2019. Chronotherapy for hypertension: improvement in patient outcomes with bedtime administration of antihypertensive drugs. Eur. Heart J.

[31] Portaluppi, F., Hermida, R.C., 2007. Circadian rhythms in cardiac arrhythmias and opportunities for their chronotherapy. Adv. Drug Deliv. Rev. 59 (9–10), 940–951.

[32] Burioka, N., Sako, T., Tomita, K., Miyata, M., Suyama, H., Igishi, T., Shimizu, E., 2000. Theophylline chronotherapy of nocturnal asthma using bathyphase of circadian rhythm in peak expiratory flow rate. Biomed. Pharmacother. 55, s142–s146.

[33] Li, X., Lu, C., Yang, Y., Yu, C., Rao, Y., 2020. Site-specific targeted drug delivery systems for the treatment of inflammatory bowel disease. Biomed. Pharmacother. 129, 110486.

[34] Linares, V., Casas, M., Caraballo, I., 2019. Printfills: 3D printed systems combining fused deposition modeling and injection volume filling. application to colon-specific drug delivery. Eur. J. Pharm. Biopharm. 134, 138–143.

[35] Goyanes, A., Chang, H., Sedough, D., Hatton, G.B., Wang, J., Buanz, A., Gaisford, S., Basit, A.W., 2015. Fabrication of controlled-release budesonide tablets via desktop (FDM) 3D printing. Int. J. Pharm. 496 (2), 414–420.